

## Research Article

# High Improvement in Conversion Efficiency of $\mu\text{c-SiGe}$ Thin-Film Solar Cells with Field-Enhancement Layers

Shu-Hung Yu,<sup>1</sup> Wei Lin,<sup>1</sup> Yu-Hung Chen,<sup>2</sup> and Chun-Yen Chang<sup>1</sup>

<sup>1</sup>Department of Electronics Engineering and Institute of Electronics, National Chiao Tung University, Hsinchu 30010, Taiwan

<sup>2</sup>Photovoltaic Technology Division, Green Energy and Environment Research Laboratories, Industrial Technology Research Institute, Hsinchu 31040, Taiwan

Correspondence should be addressed to Chun-Yen Chang, cycassist@gmail.com

Received 20 January 2012; Accepted 19 February 2012

Academic Editor: David Lee Phillips

Copyright © 2012 Shu-Hung Yu et al. This is an open access article distributed under the Creative Commons Attribution License, which permits unrestricted use, distribution, and reproduction in any medium, provided the original work is properly cited.

The improved performance for hydrogenated microcrystalline silicon-germanium ( $\mu\text{c-Si}_{1-x}\text{Ge}_x\text{:H}$ ,  $x \sim 0.1$ ) p-i-n single solar cells with hydrogenated microcrystalline silicon ( $\mu\text{c-Si:H}$ ) field-enhancement layers (FELs) is demonstrated for the first time. The fill factor (FF) and conversion efficiency ( $\eta$ ) increase by about 19% and 28% when the thickness of the  $\mu\text{c-Si}$  FEL is increased from 0 to 200 nm, it is attributed to the longer hole life-time and enhanced electric field in the  $\mu\text{c-Si}_{0.9}\text{Ge}_{0.1}\text{:H}$  layer. Therefore, we can successfully manufacture high-performance  $\mu\text{c-SiGe:H}$  solar cells with the thickness of absorbers smaller than 1  $\mu\text{m}$  by conducting FELs. Moreover, the simulation tool is used to simulate the current-voltage ( $J$ - $V$ ) curve, thus we can investigate the carrier transport in the absorber of  $\mu\text{c-Si}_{0.9}\text{Ge}_{0.1}\text{:H}$  solar cells with different EFLs.

## 1. Introduction

In order to enhance the infrared absorption of thin-film solar cells, many efforts have been developed such as textured substrates or alloy absorbers. Textured substrates efficiently scatter incoming light and increase the optical length in absorbers [1]. However, rough morphology of the substrates can induce many cracks in absorption layers and damage the photocarrier transport [2]. The alternative methods, that is, high absorption coefficient alloy absorbers such as hydrogenated microcrystalline silicon-germanium ( $\mu\text{c-Si}_{1-x}\text{Ge}_x\text{:H}$ ), have been developed for thin-film solar cells [3]. It has been reported that light absorption coefficient of  $\mu\text{c-Si}_{1-x}\text{Ge}_x\text{:H}$  films can be enhanced about from  $4 \times 10^2$  to  $4 \times 10^3 \text{ cm}^{-1}$  (@ 900 nm) when the Ge content is increased from 0 to 60 at. % [4, 5]. Moreover, Takuya Matsui et al. have demonstrated that a micromorph tandem cell with a  $\mu\text{c-Si}_{1-x}\text{Ge}_x\text{:H}$  ( $x = 0.1$ ) bottom cell can reveal an initial conversion efficiency of 11.2% [6]. However, the incorporation of Ge may induce strain defects, dangling bond defects [7, 8], and acceptor-like states [4], hence it can result in reduced electric field in the absorbers.

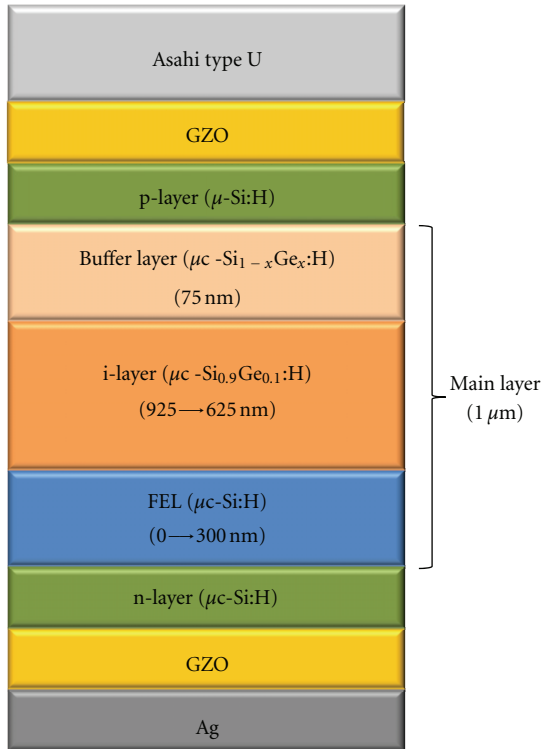
Here, hydrogenated microcrystalline silicon ( $\mu\text{c-Si:H}$ ) field-enhancement layers (FELs) are developed to improve the performance of  $\mu\text{c-Si}_{1-x}\text{Ge}_x\text{:H}$  p-i-n single solar cells for the first time, and we optimize the thickness of the FEL based on the conversion efficiency. Moreover, Atlas device simulator from SILVACO company is used to simulate the current-voltage curve of thin film solar cells. We analyze the band diagram and electric field in the device, the simulation results demonstrate that the FEL can enhance the hole life-time and electric field in the  $\mu\text{c-Si}_{0.9}\text{Ge}_{0.1}\text{:H}$  absorber.

## 2. Device Fabrication

In this study, superstrate-type  $\mu\text{c-Si}_{1-x}\text{Ge}_x\text{:H}$  single cells are fabricated on Asahi type- $U$  glass substrates by a 40 MHz plasma enhanced chemical vapor deposition (PECVD) system. The single cell consists of Asahi type- $U$  glass/ $\text{ZnO:Ga(GZO)}/\text{p-}\mu\text{c-Si:H}/\mu\text{c-Si}_{1-x}\text{Ge}_x\text{:H}$  buffer layer/ $i\text{-}\mu\text{c-Si}_{0.9}\text{Ge}_{0.1}\text{:H}/\mu\text{c-Si:H}$  FEL/ $n\text{-}\mu\text{c-Si:H}/\text{GZO}/\text{Ag}$ . The schematic diagram is shown in Figure 1. The buffer layer is graded intrinsic  $\mu\text{c-Si}_{1-x}\text{Ge}_x\text{:H}$  and its thickness is about 75 nm, it is obtained by varying hydrogen-diluted (10%)  $\text{GeH}_4$  gas flow

TABLE 1: Material parameters.

Parameters	$\mu\text{c-Si}_{0.9}\text{Ge}_{0.1}\text{:H}$				$\mu\text{c-Si:H}$
	FEL = 0 nm	FEL = 100 nm	FEL = 200 nm	FEL = 300 nm	
Optical gap (eV)		1.24			1.3
Elec. mob. ( $\text{cm}^2/\text{Vs}$ )		20			30
Hole mob. ( $\text{cm}^2/\text{Vs}$ )		2			2
Con. Band DOS ( $\text{cm}^{-3}$ )		$1 \times 10^{20}$			$1 \times 10^{20}$
Val. Band DOS ( $\text{cm}^{-3}$ )		$1 \times 10^{20}$			$1 \times 10^{20}$
Hole life-time (s)	$5.0 \times 10^{-10}$	$1.2 \times 10^{-9}$	$1.7 \times 10^{-9}$	$8.0 \times 10^{-10}$	$1 \times 10^{-7}$
Tail states density factor:					
Con. Band ( $\text{cm}^{-3}/\text{eV}$ )	$5.0 \times 10^{19}$	$5.2 \times 10^{19}$	$5.3 \times 10^{19}$	$5.6 \times 10^{19}$	$1.0 \times 10^{19}$
Val. Band ( $\text{cm}^{-3}/\text{eV}$ )	$5.0 \times 10^{19}$	$5.2 \times 10^{19}$	$5.2 \times 10^{19}$	$5.3 \times 10^{19}$	$1.0 \times 10^{19}$
Tail states charact. energy:					
Con. Band (eV)		0.027			0.027
Val. Band (eV)		0.045			0.045
Acceptor-like Gaussian defect states:					
Below con. band (eV)		0.4			0.4
Decay energy (eV)		0.2			0.2
DOS ( $\text{cm}^{-3}/\text{eV}$ )	$7.0 \times 10^{16}$	$7.0 \times 10^{16}$	$7.0 \times 10^{16}$	$7.1 \times 10^{16}$	$1.0 \times 10^{15}$
Donor-like Gaussian defect states:					
Above val. band (eV)		0.45			0.45
Decay energy (eV)		0.2			0.2
DOS ( $\text{cm}^{-3}/\text{eV}$ )		$7.0 \times 10^{16}$			$1.0 \times 10^{15}$

FIGURE 1: Schematic diagram of the  $\mu\text{c-Si}_{0.9}\text{Ge}_{0.1}\text{:H}$  p-i-n solar cell with the graded  $\mu\text{c-Si}_{1-x}\text{Ge}_x\text{:H}$  buffer layer and  $\mu\text{c-Si:H}$  FEL.

rate ( $[\text{GeH}_4]$ ) from 0 to 4 sccm under a constant  $\text{SiH}_4$  gas flow rate ( $[\text{SiH}_4]$ ) of 17 sccm. The  $i\text{-}\mu\text{c-Si}_{0.9}\text{Ge}_{0.1}\text{:H}$  absorber is deposited at a fixed  $[\text{GeH}_4]$  of 5 sccm and an  $[\text{SiH}_4]$  of 17 sccm. The  $\mu\text{c-Si:H}$  FEL is grown at a constant  $[\text{SiH}_4]$  of 20 sccm and its thickness is varied from 0 to 300 nm. The main layer of solar cells consists of the buffer layer, the absorber, and the FEL and the total thickness is kept  $1 \mu\text{m}$ .

The Raman spectra are performed by Confocal Raman Microscope (HORIBA, LabRAM HR) at room temperature in the backscattering configuration. The source light is Helium-Neon (HeNe) laser emitting at a wavelength of 632.8 nm. The Ge content of  $\mu\text{c-Si}_{1-x}\text{Ge}_x\text{:H}$  films can be identified from the Raman spectra. Edge isolation is conducted by the laser scriber to define the device area of  $1.0 \text{ cm}^2$ . The current-voltage ( $J$ - $V$ ) characteristics of solar cells are measured under an Air Mass 1.5 Global (AM 1.5 G) spectrum with an irradiation of  $100 \text{ mW}/\text{cm}^2$  by a solar simulator.

We use Atlas to calculate internal electrical characteristics of solar cells in the one-dimension (perpendicular to the substrate). The simulation is based on  $J$ - $V$  measurement results. Here, Newton method is used to solve Poisson's and continuity equations for the steady state. The carrier occupation and recombination in the forbidden gap states are considered by the Shockley-Read-Hall (SRH) recombination model. Table 1 shows the basic parameters in the  $\mu\text{c-Si}_{0.9}\text{Ge}_{0.1}\text{:H}$  and  $\mu\text{c-Si:H}$  layers.

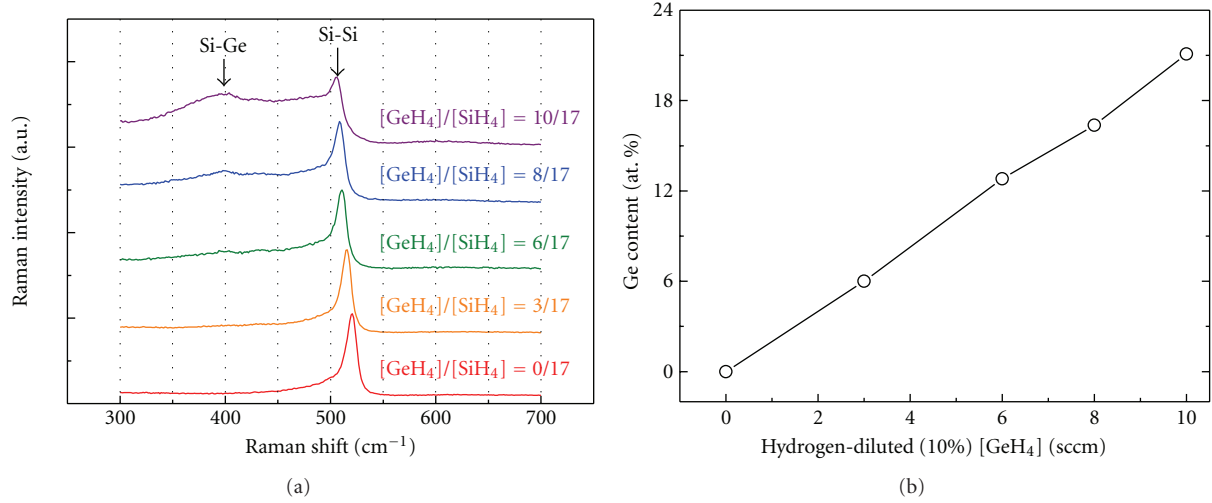


FIGURE 2: (a) Raman spectra of  $\mu\text{c-Si}_{1-x}\text{Ge}_x\text{:H}$  films deposited at different  $[\text{GeH}_4]/[\text{SiH}_4]$  ratios. (b) The Ge content of  $\mu\text{c-Si}_{1-x}\text{Ge}_x\text{:H}$  films deposited at different  $[\text{GeH}_4]$  estimated from Raman spectra.

### 3. Results and Discussion

Raman spectra of  $\mu\text{c-Si}_{1-x}\text{Ge}_x\text{:H}$  deposited at different gas flow rates ( $[\text{GeH}_4]$ : 0–10 sccm,  $[\text{SiH}_4]$ : 17 sccm) are presented in Figure 2(a). When the Ge content of  $\mu\text{c-Si}_{1-x}\text{Ge}_x\text{:H}$  films is increased, the main peak ( $\omega_{\text{Si-Si}}$ ) corresponding to the Si-Si transverse optical (TO) mode in the crystalline phase will gradually be lower than  $520\text{ cm}^{-1}$  and the peak near  $400\text{ cm}^{-1}$  attributed to Si-Ge bond will be apparent. The relation between the Ge content and  $\omega_{\text{Si-Si}}$  is depicted as [6]:  $\omega_{\text{Si-Si}} = 520 - 70x$ . Figure 2(b) shows the nearly linear relation between the Ge content of  $\mu\text{c-Si}_{1-x}\text{Ge}_x\text{:H}$  films and the  $\text{GeH}_4$  gas flow rate, hence we can estimate the Ge content of the absorber at about 10 at. %.

$J$ - $V$  measurement and simulation curves of  $\mu\text{c-Si}_{0.9}\text{Ge}_{0.1}\text{:H}$  solar cells with different  $\mu\text{c-Si:H}$  FELs are shown in Figure 3. The inserted table shows the  $J$ - $V$  parameters of  $\mu\text{c-Si}_{0.9}\text{Ge}_{0.1}\text{:H}$  solar cells. When the thickness of the FEL is widened from 0 to 200 nm, the open-circuit voltage ( $V_{\text{oc}}$ ) is increased from 0.433 to 0.453 V and the short-circuit current density ( $J_{\text{sc}}$ ) is enhanced from 20.8 to 21.5  $\text{mA}/\text{cm}^2$ . In addition, the fill factor (FF) is enhanced from 47.3 to 56.4% and conversion efficiency ( $\eta$ ) is enhanced from 4.3 to 5.5%. Quantum efficiency (QE) spectra of  $\mu\text{c-Si}_{0.9}\text{Ge}_{0.1}\text{:H}$  solar cells (FEL = 0, 200 nm) at a reverse bias of 0 and  $-0.5\text{ V}$  are shown in Figure 4. Under a reverse bias of 0 and  $-0.5\text{ V}$ , QE spectra of the  $\mu\text{c-Si}_{0.9}\text{Ge}_{0.1}\text{:H}$  solar cell without FEL are divided apparently. However, the  $\mu\text{c-Si}_{0.9}\text{Ge}_{0.1}\text{:H}$  solar cell with the 200 nm FEL exhibits more matching QE spectra in the wavelength range of 500–800 nm. This result implies that the  $\mu\text{c-Si}_{0.9}\text{Ge}_{0.1}\text{:H}$  solar cell equipping with the FEL has the enhanced electric field in the  $\mu\text{c-Si}_{0.9}\text{Ge}_{0.1}\text{:H}$  layer. However, the FF and  $\eta$  decrease to 53.4% and 5.1% when the FEL rises to 300 nm, but  $V_{\text{oc}}$  and  $J_{\text{sc}}$  do not suffer severely. Consequently, we found that 200 nm is the optimized thickness of the FEL for solar cell.

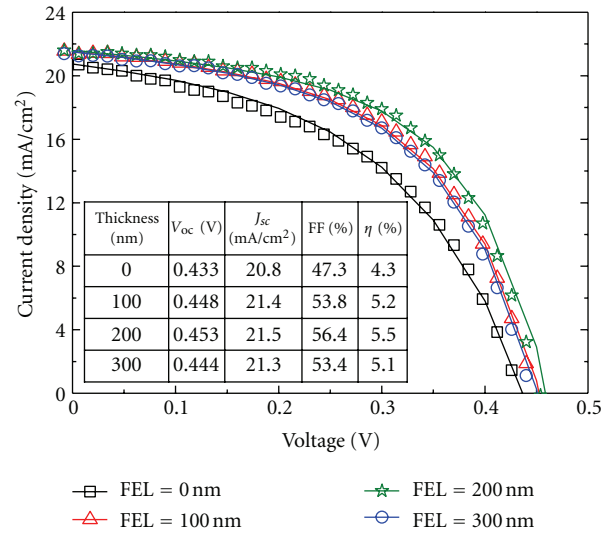


FIGURE 3:  $J$ - $V$  measurements of  $\mu\text{c-Si}_{0.9}\text{Ge}_{0.1}\text{:H}$  solar cells with  $\mu\text{c-Si:H}$  FEL varied from 0 to 300 nm.

Figure 5 (a) shows the band diagram in the main layer of the solar cell in thermodynamic equilibrium. Because the optical band gap of  $\mu\text{c-Si:H}$  is higher than one of  $\mu\text{c-Si}_{0.9}\text{Ge}_{0.1}\text{:H}$ , there must be a valence-band discontinuity in the p-i interface and the hole extraction might be block. Graded  $\mu\text{c-Si}_{1-x}\text{Ge}_x\text{:H}$  buffer layers are conducted to reduce this energy discontinuity and enhance the hole transport. Around the interface between the  $\mu\text{c-Si}_{0.9}\text{Ge}_{0.1}\text{:H}$  and the  $\mu\text{c-Si:H}$  FEL, the energy barrier seen by hole carriers can repel it and reduce recombination probability near the back side of the main layer. The simulation results based on the Shockley-Read-Hall (SRH) recombination model show that hole life-time can be enhanced from  $5 \times 10^{-10}$  to  $1.7 \times 10^{-9}\text{ s}$  when the FEL is increased from 0 to 200 nm. Figure 5(b)

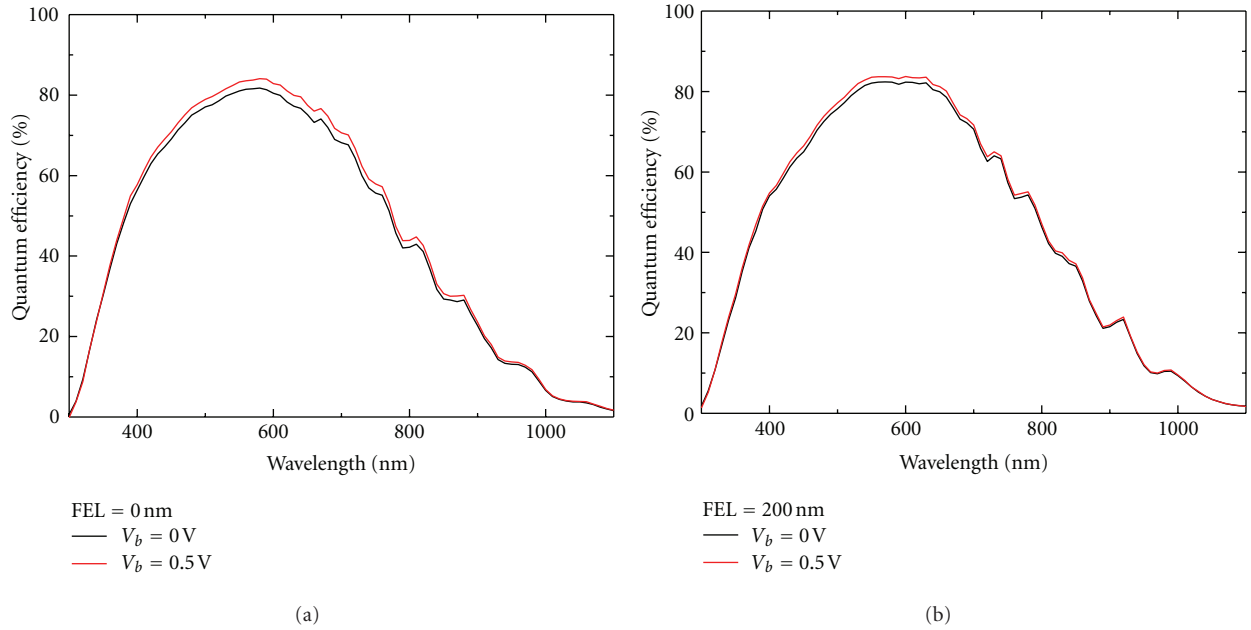


FIGURE 4: (a) QE spectra of the  $\mu\text{c-Si}_{0.9}\text{Ge}_{0.1}\text{:H}$  solar cell without FEL and (b) with FEL of 200 nm at a reverse bias of 0 and  $-0.5\text{ V}$ .

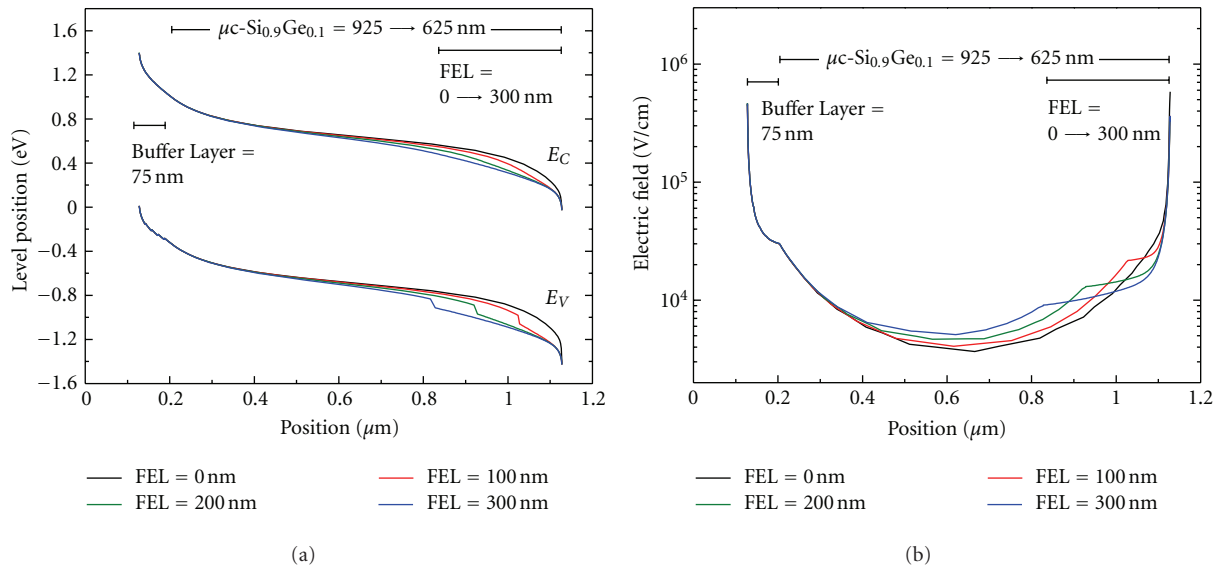


FIGURE 5: (a) The band diagram and (b) the electric field in the main layer of the solar cell with different  $\mu\text{c-Si:H}$  FEL in thermodynamic equilibrium.

shows the electric field of the main layer in thermodynamic equilibrium. When the thickness of the FEL is increased from 0 to 200 nm, the electric field in the  $\mu\text{c-Si}_{0.9}\text{Ge}_{0.1}\text{:H}$  layer can be enhanced significantly. This is because that  $\mu\text{c-Si:H}$  has lower defect density than  $\mu\text{c-Si}_{0.9}\text{Ge}_{0.1}\text{:H}$  and the field-screening effect related to trapped charges can be reduced efficiently. The enhanced electric field in the  $\mu\text{c-Si}_{0.9}\text{Ge}_{0.1}\text{:H}$  layer is useful for photocarrier extraction. The electric field in the  $\mu\text{c-Si}_{0.9}\text{Ge}_{0.1}\text{:H}$  layer can be increased further when we widen the FEL from 200 to 300 nm. However, the electric field in the thick FEL is decreased significantly. Additionally, we observe that hole life-time is reduced to  $8 \times 10^{-10}\text{ s}$  when

the FEL is 300 nm. This result is probably due to the poor crystallinity in a thinner  $\mu\text{c-Si}_{0.9}\text{Ge}_{0.1}\text{:H}$  layer. Hence, we speculate that diminished hole life-time and reduced electric field in the thick FEL result in the degraded performance of the solar cell.

#### 4. Conclusion

High-performance  $\mu\text{c-Si}_{0.9}\text{Ge}_{0.1}\text{:H}$  single cells with the absorber smaller than  $1\ \mu\text{m}$  are achieved by equipping with  $\mu\text{c-Si:H}$  FELs. We use  $\mu\text{c-Si:H}$  FELs and graded  $\mu\text{c-Si}_{1-x}\text{Ge}_x\text{:H}$  buffer layers to improve the photocarrier

transport in the  $\mu\text{c-Si}_{0.9}\text{Ge}_{0.1}\text{:H}$  layers. The Ge composition of  $\mu\text{c-Si}_{1-x}\text{Ge}_x\text{:H}$  films can be evaluated quantitatively from Raman spectra. When we widen the thickness of the FEL from 0 to 200 nm,  $V_{\text{oc}}$  is enhanced from 0.433 to 0.453 V and  $J_{\text{sc}}$  is enhanced from 20.8 to 21.5 mA/cm<sup>2</sup>. Moreover, FF and  $\eta$  approximately exhibit 19% and 28% enhancements. It is attributed to the improved electric field and longer hole lifetime in the  $\mu\text{c-Si}_{1-x}\text{Ge}_x\text{:H}$  layer. However, FF and  $\eta$  are both decreased when the thickness of the FEL exceeds 200 nm. This is due to poor crystalline  $\mu\text{c-Si}_{0.9}\text{Ge}_{0.1}\text{:H}$  layer and the reduced electric field in the thick FEL. There is a trade-off between the enhanced electric field in the absorber and the reduced one in the FEL.

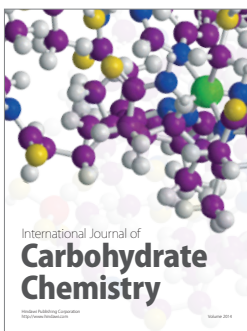
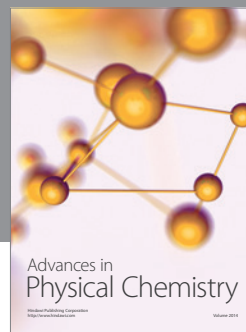
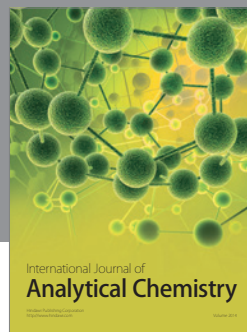
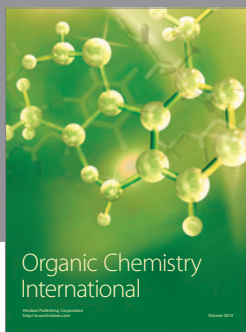
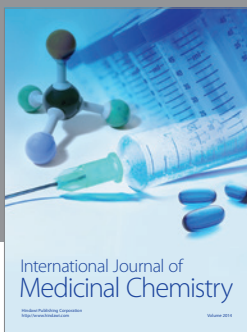
## Acknowledgment

This work was supported by the National Science Council of Taiwan under Grant NSC 100-3113-E-009-004, and Bureau of Energy, Ministry of Economic Affairs, Taiwan, under Grant no. A455DR1110.

## References

- [1] A. Hongsingthong, T. Krajangsang, I. A. Yunaz, S. Miyajima, and M. Konagai, "ZnO films with very high haze value for use as front transparent conductive oxide films in thin-film silicon solar cells," *Applied Physics Express*, vol. 3, no. 5, Article ID 051102, 2010.
- [2] C. Battaglia, J. Escarré, K. Söderström et al., "Nanoimprint lithography for high-efficiency thin-film silicon solar cells," *Nano Letters*, vol. 11, no. 2, pp. 661–665, 2011.
- [3] G. Ganguly, T. Ikeda, T. Nishimiya, K. Saitoh, M. Kondo, and A. Matsuda, "Hydrogenated microcrystalline silicon germanium: a bottom cell material for amorphous silicon-based tandem solar cells," *Applied Physics Letters*, vol. 69, no. 27, pp. 4224–4226, 1996.
- [4] T. Matsui, M. Kondo, K. Ogata, T. Ozawa, and M. Isomura, "Influence of alloy composition on carrier transport and solar cell properties of hydrogenated microcrystalline silicon-germanium thin films," *Applied Physics Letters*, vol. 89, no. 14, Article ID 142115, 2006.
- [5] A. V. Shah, H. Schade, M. Vanecsek et al., "Thin-film silicon solar cell technology," *Progress in Photovoltaics: Research and Applications*, vol. 12, no. 2-3, pp. 113–142, 2004.
- [6] T. Matsui, H. Jia, and M. Kondo, "Thin film solar cells incorporating microcrystalline  $\text{Si}_{1-x}\text{Ge}_x$  as efficient infrared absorber: an application to double junction tandem solar cells," *Progress in Photovoltaics: Research and Applications*, vol. 18, no. 1, pp. 48–53, 2010.
- [7] T. Matsui, C. W. Chang, T. Takada, M. Isomura, H. Fujiwara, and M. Kondo, "Microcrystalline  $\text{Si}_{1-x}\text{Ge}_x$  solar cells exhibiting enhanced infrared response with reduced absorber thickness," *Applied Physics Express*, vol. 1, no. 3, pp. 0315011–0315013, 2008.
- [8] Y. H. Chen, H. Y. Fang, and C. M. Yeh, "Raman scattering and electrical characterizations studies of hydrogenated amorphous silicon-germanium alloys prepared by 40 MHz plasma-enhanced CVD," *Journal of Non-Crystalline Solids*, vol. 357, no. 1, pp. 1–3, 2011.





# Hindawi

Submit your manuscripts at  
<http://www.hindawi.com>

